Supplementary Information

Sensitive label free imaging of 3D cell models with minimal toxicity using confocal reflectance

Michael A. Taylor*, Jung Un Ally Choi*, Shiva Muthuswamy, Marco A. Enriquez Martinez, Jan Lauko, Amanda W. Kijas, Alan E. Rowan

Australian Institute for Bioengineering and Nanotechnology, The University of Queensland, St. Lucia, Queensland 4072, Australia.

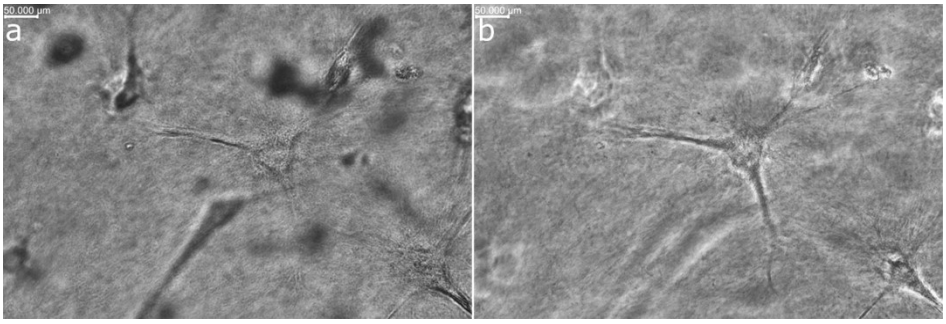

Supplementary Fig. 1. Standard label-free imaging methods in a 3D culture. (a) Bright field and (b) phase contrast imaging of a fibroblast embedded in 3D collagen both provide poor image quality in 3D.

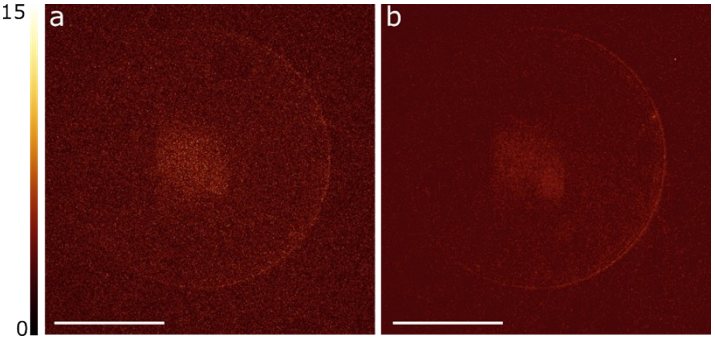

Supplementary Fig. 2. Background reflectance. (a) Background reflectance in MilliQ water. The pattern seen here is an artifact resulting from stray reflection within the microscope and is commonly seen in confocal reflectance[12]. This is not visible in fluorescence imaging as the emission filter removes any reflected excitation light. The artifact is present in all results, but in most of our images is difficult to see as it is substantially less bright than any of the cellular features presented here. The background here is recorded with higher power than the main text results (10% here, c.f. 2–4% in main text), and brightness scale increased to make the faint background visible. Mean is 3.4 counts. (b) The background in PIC, with no added sample, is similarly faint enough for the microscope reflectance to dominate background from the sample. Scale bar: 50 µm.

Comment [SM]: c.f needs to be defined

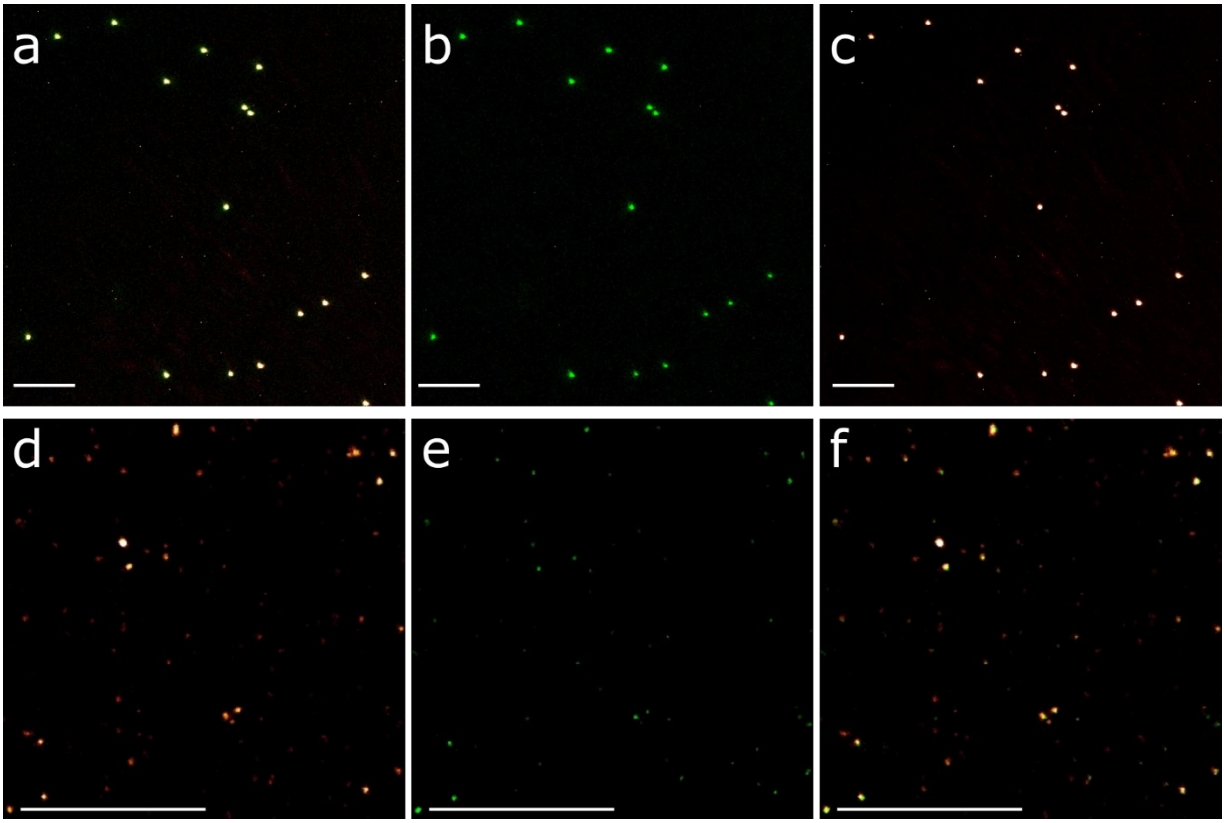

Supplementary Fig. 3. Fluorescent nanospheres of diameter 250 nm (a–c) and 50 nm (d–f) were imaged with reflectance (a, d) and fluorescence (b, e), with overlays shown in (c, f), (maximum intensity projections). For 250 nm nanospheres, there is near-perfect agreement between reflectance and fluorescence. For 50 nm, each fluorescent spot is also visible in the reflectance. However, we also see some additional background scattering with reflectance, likely from small impurities in the sample. The signal from 50 nm nanospheres is very faint, such that imaging is highly sensitive to the smallest impurities in the sample. Scale bars: 10 µm.

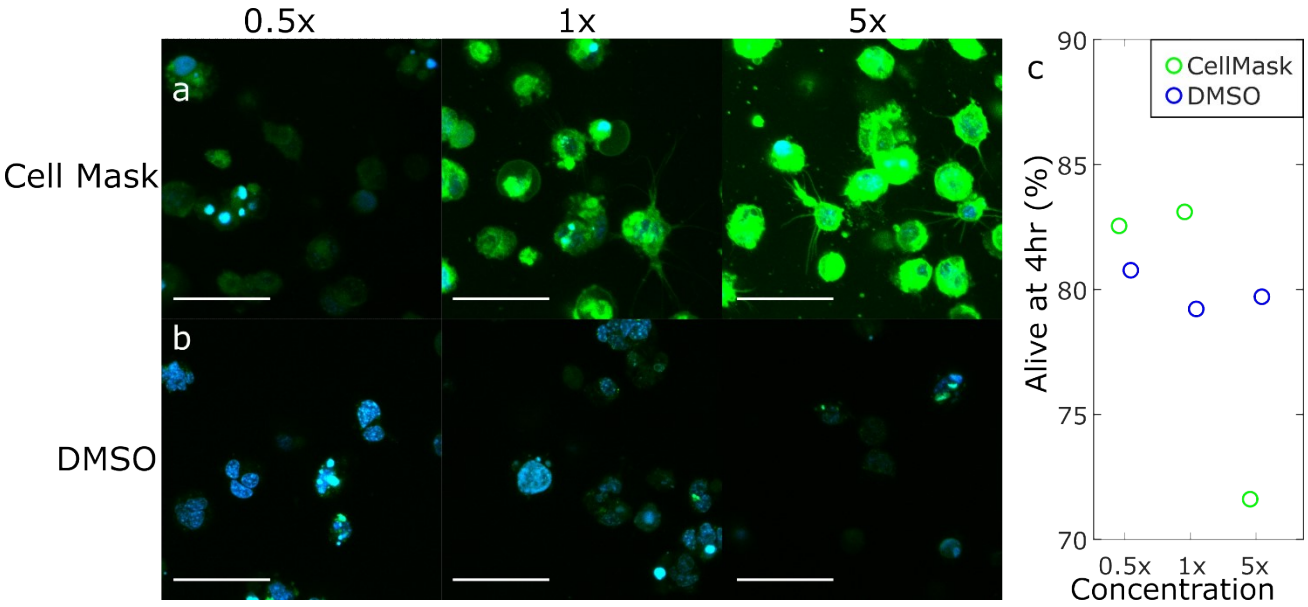

Supplementary Fig. 4. Titration of CellMask™. In order to establish an appropriate concentration and incubation time to permit observation of dendrites with fluorescence confocal microscopy, we tested the imaging and cell viability at different concentrations of CellMask™. (a) Fluorescence images with CellMask™ (green) and Hoechst (blue) recorded 3 hours after staining, with different concentrations of CellMask™ of 2.5 µg/mL (0.5x), 5 µg/mL (1x), and 25 µg/mL (5x). (b) As a control we imaged cells stained with Hoechst in similar concentrations of DMSO. The cell viability was measured using propidium iodide live/dead staining. The fluorescent wavelength of CellMask™ and propidium iodide overlap, which led to cross-talk in the fluorescence channels. To distinguish propidium iodide from spurious CellMask™ fluorescence, we note that propidium iodide localizes in the cell nucleus of dead cells. Hence cells were deemed dead if the fluorescence localized in the nucleus. (c) The proportion of cells that were alive for each of the 6 conditions. We see increased cell death at 5x concentration of CellMask™, with no clear evidence of damage at the other conditions. Based on these results, for our live imaging experiments we used 5 µg/mL concentration of CellMask™, and 4 hours of incubation, as this allows clear imaging of dendrites without excessive cell death. Scale bars: 50 µm.

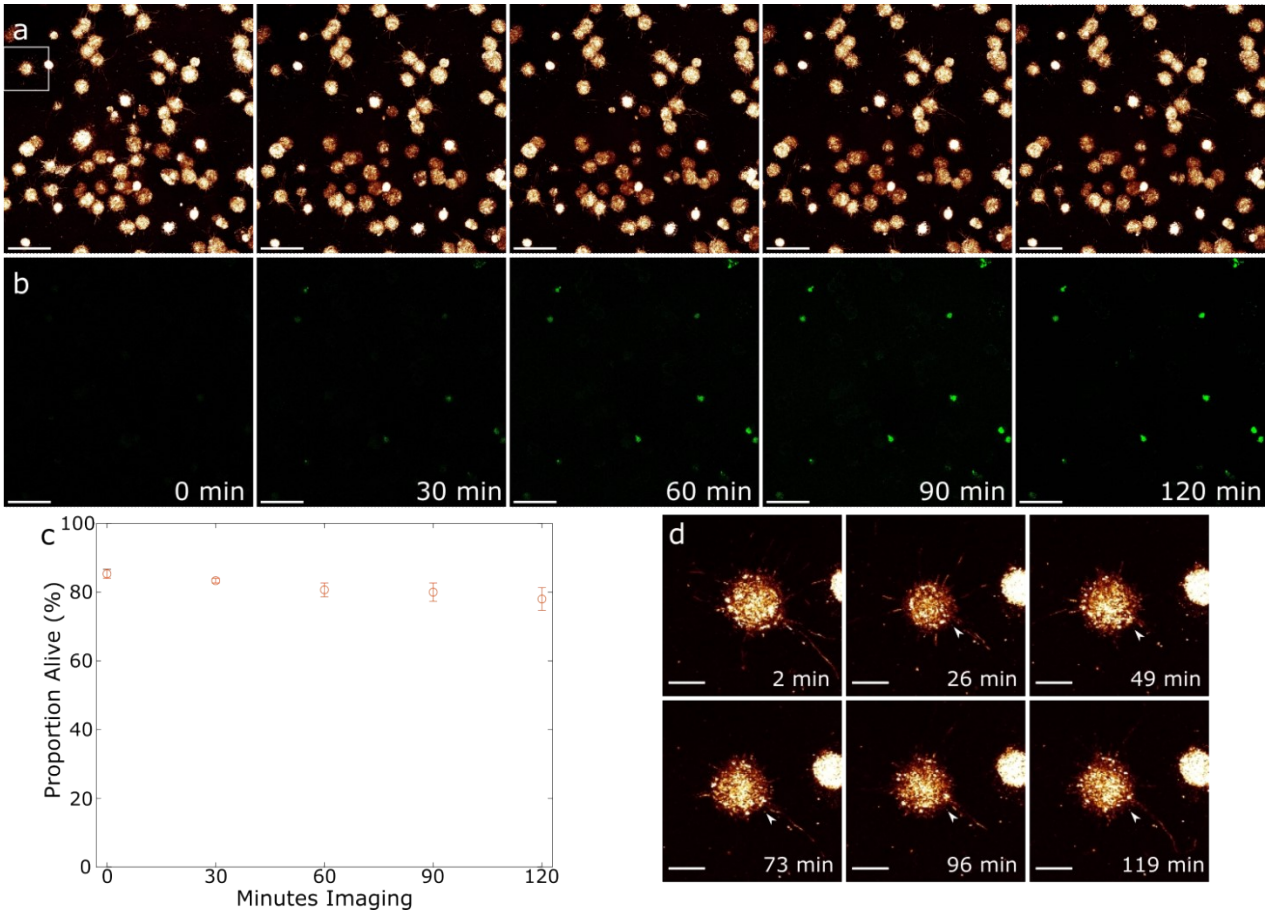

Supplementary Fig. 5. Viability of cells in long term confocal reflectance imaging. A population of osteocytes in PIC hydrogel was imaged for 2 hours, with the imaging broken into four 29 minute blocks of continuous imaging. The full video is included in Supplementary Video 3. To assess the appearance of photodamage, cell viability was assessed using NucGreen™ imaging before imaging, and after each 29 minute block. The viability assessment required a further 1 minute of laser exposure, so these cells were exposed for a total of 2 hours. (a) Reflectance images of osteocytes in PIC hydrogel, and (b) corresponding NucGreen™ live/dead images. While the brightness of the NucGreen™ stained cells increases over time, most of the cells that are later identified as dead are already fluorescent in the initial image. As such, these cells were non-viable prior to imaging, and do not indicate any toxicity from reflectance imaging. (c) Proportion of the cells which are considered alive (n=2). We see a small but significant (7%) reduction in cell viability over the 2 hours of imaging. (d) A zoom in on the cell highlighted in (a). In addition to the movement of dendrites, as discussed in Fig. 2, we can also see a small spot appear at the cell surface, which then appears to become immobilized in the nearby matrix (arrows). Scale bars: 50 µm (a, b), 10 µm (d).

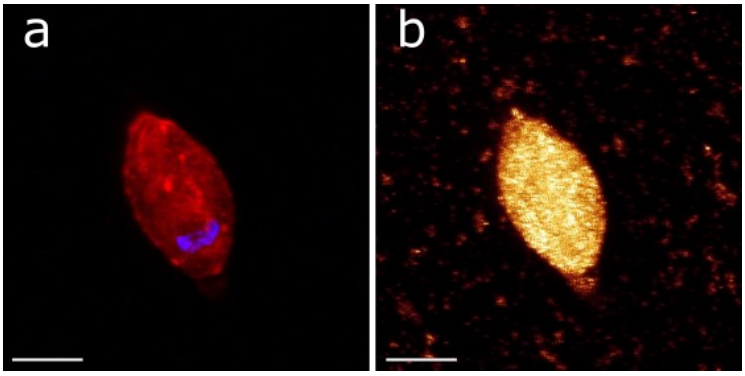

Supplementary Fig. 6. Confocal reflectance imaging in hyaluronic acid. (a) Fibroblast, stained with DAPI (nucleus, blue) and SiR-Actin (actin, red). (b) Corresponding confocal reflectance image. While we see numerous background spots, the background level is overall very low. Compared to fibroblasts in collagen, PIC, and fibrin, the morphology seen here is very different and more rounded. This may be caused by the low mechanical stiffness of the matrix. Scale bars: 20 µm.

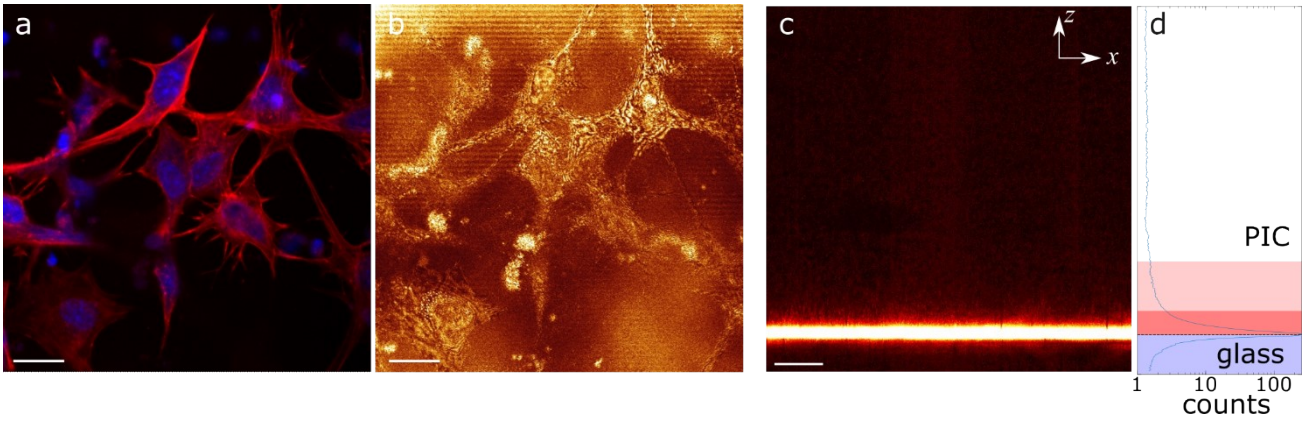

Supplementary Fig. 7. Confocal reflectance in 2D. (a) Osteocytes on a 2D surface, stained with DAPI (nucleus, blue) and phalloidin (actin, red). (b) Corresponding confocal reflectance image. The coverslip produces a large reflection that far exceeds the scattering from cells. However, we can see interference between the scattered light and the flat glass surface, which permits measurement of nanostructure with very low power. Since this relies on interference, we see bright and dark fringes as the cell thickness varies, causing the scattered light to alternate between contributing constructive and destructively. Recent work demonstrated that with appropriate analysis this interference can be used to provide quantitative phase measurement[19]. (c) An x–z plane image of confocal reflectance around the coverslip surface in a control PIC sample, with (d) the average number of counts at different depths. Within 10 µm of the glass surface, the reflection from glass is brighter than the signals from cells. The reflection from the coverslip is minimal at 20 µm from the glass surface. At depths greater than around 40 µm from the glass surface, the reflection from the coverslip was not measurable in our system. Scale bars: 20 µm.

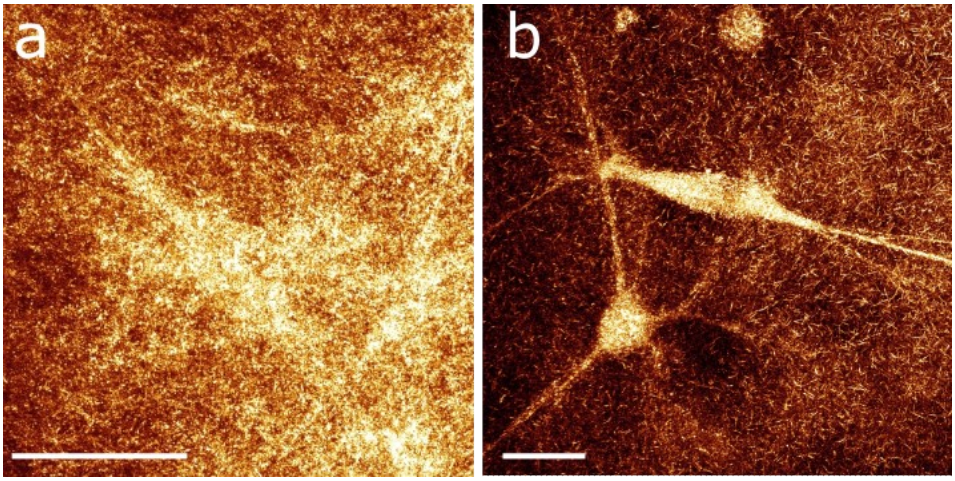

Supplementary Fig. 8. Confocal reflectance imaging in collagen gels with different architecture. The background produced by the collagen varies considerably with the network architecture, which itself depends crucially on the preparation procedure. Here the collagen is prepared (a) with a fine mesh of 2 µm pore size, and (b) a coarse 7 µm pore size. Scale bars: 50 µm.

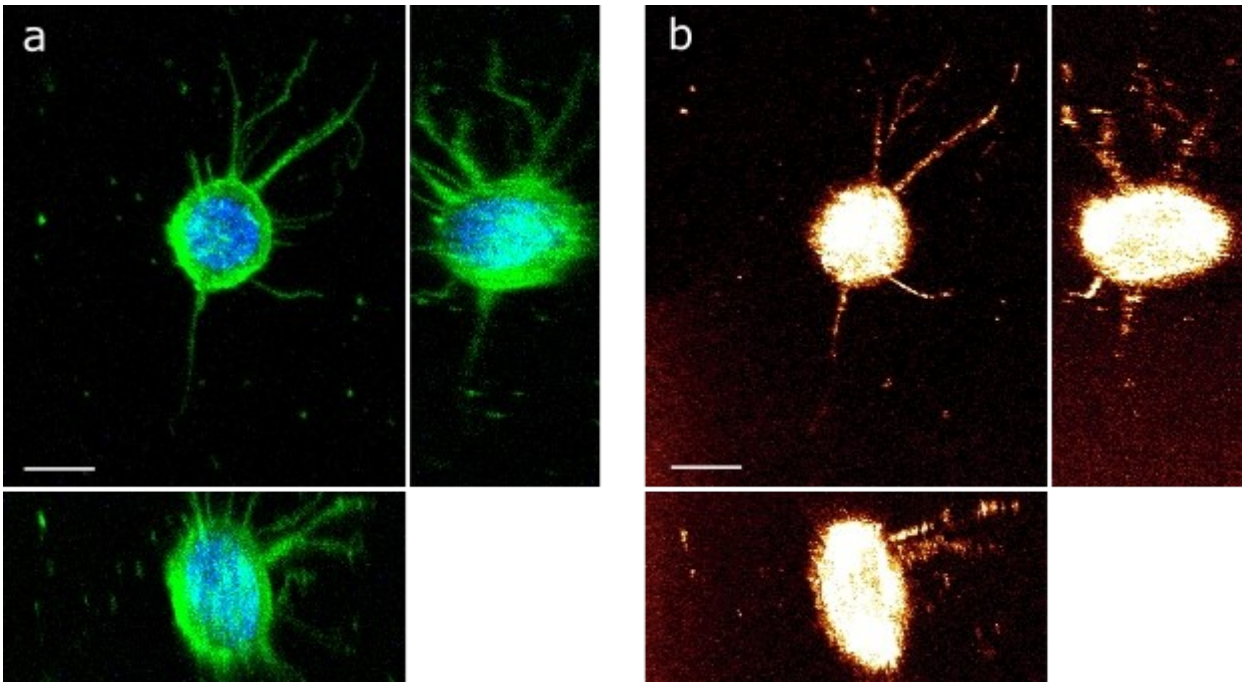

Supplementary Fig. 9. Maximum intensity projections along the x, y, and z axes. (a) An osteocyte cell stained with DAPI (blue) and CellMask™. (b) Corresponding reflectance images. While the lateral dendrites are well sampled with reflectance, the vertically aligned dendrites visible with CellMask™ are not seen in reflectance imaging. Scale bars: 10 µm.

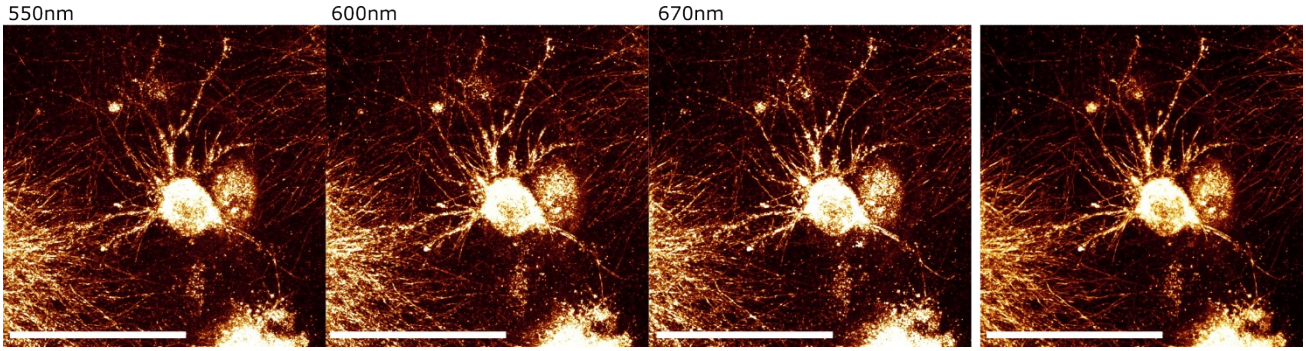

Supplementary Fig. 10. Reflectance images taken at (a) 550 nm, (b) 600 nm, (c) 670 nm, and (d) the mean of the three images. Each wavelength has had colour scale adjusted to provide comparable brightness. Averaging over multiple wavelengths smooths the speckle artifacts that are visible with confocal reflectance imaging. Scale bars: 50 µm.

Supplementary Note 1

Interestingly, we observed punctate signals in the hydrogel surrounding the cells (Fig. 3e of the main text), which were not present in cell-free PIC hydrogel samples (see Supplementary Fig. 2b). The punctuate objects co-stained with membrane marker and a common osteocyte transmembrane protein, E11/podoplanin that is important for the dendritic formation[23] (Fig. 3f of main text). We tentatively identify these small objects as vesicles. Long-term time lapse cell imaging shows such objects appearing to emerge from the cell surface (Supplementary Fig. 5d). While existing label-free imaging methods such as phase contrast microscopy can visualize vesicle release in 2D cell cultures[24], our method additionally constrains the motion of released vesicles, allowing immunostaining to characterise and quantify vesicle contents following release. There are no other existing methods that combine the capacity for stain-free live imaging with immunostaining-based characterization of protein contents. As shown in Supplementary Fig. 3, confocal reflectance imaging provides sufficient sensitivity to image fluorescent nanospheres with diameters as small as 50 nm. Most extracellular vesicles are larger than 50 nm and so could be detectable using confocal reflectance[25], though smaller particles would not be detectable and the contrast and the sensitivity of the vesicles could vary with respect to their sizes

Supplementary References

23. Nakamura, T.M. *et al.* Podoplanin is dispensable for mineralized tissue formation and maintenance in the Swiss outbred mouse background. *Genesis* **59**, e23450 (2021).
24. Levy, D., Do, M.A., Zhang, J., Brown, A. & Lu, B. Orchestrating Extracellular Vesicle With Dual Reporters for Imaging and Capturing in Mammalian Cell Culture. *Frontiers in Molecular Biosciences* **8**, 680580 (2021).
25. Van Niel, G., d'Angelo, G., Raposo, G. Shedding light on the cell biology of extracellular vesicles, *Nat. Rev. Mol. Cell Biol.*, **19** 213 (2018).

Supplementary Video 1. Confocal fluorescence imaging of live osteocyte cells stained with CellMask™, as shown in Fig. 2a. The brightness is adjusted to visualize the faint dendrites, which results in saturation of the cell bodies. The full volume imaged was 292×292×25 µm, 512×512×26 voxels, and was imaged every 45.3s for 80 frames, for 1 hour total continuous live imaging. The still images shown in Fig. 2a zoom in on a cell in the upper right, which showed considerable dendritic activity. The video shows the maximum intensity projection of the 3D image stacks, and is displayed at 24fps, which is 1087x speed. Scale bar: 50 µm.

Supplementary Video 2. Confocal reflectance imaging of unstained live osteocyte cells, as shown in Fig. 2b. The brightness is adjusted to visualize the faint dendrites, which results in saturation of the cell bodies. The full volume imaged was 292×292×25 µm, 512×512×26 voxels, and was imaged every 45.3s for 80 frames, for 1 hour total continuous live imaging. The still images shown in Fig. 2b zoom in on a cell in the lower left. The video shows the maximum intensity projection of the 3D image stacks, and is displayed at 24fps, which is 1087x speed. Scale bar: 50 µm.

Supplementary Video 3. A viability experiment performed with 2 hours of reflectance imaging, with still shots shown in Supplementary Fig. 3. The full volume imaged was 291×291×60 µm, 1024×1024×31 voxels, and was imaged every 54.1s for four continuous blocks of 33 frames each (29 minutes). Cell viability was assessed between each imaging block. This video combines the four imaging blocks into a single continuous recording. The video shows the maximum intensity projection of the 3D image stacks and is displayed at 24fps (1298x speed). Scale bar: 50 µm.

Supplementary Video 4. Time-lapse imaging of a live osteocyte cell stained with CellMask™ over 1 hour, showing both confocal fluorescence and reflectance imaging. The video shows the maximum intensity projection of the 3D image stacks and is displayed at 4fps (1108x speed). Scale bar: 20 µm.